

## RESEARCH ARTICLE

WILEY

# Hepatitis B virus envelope proteins can serve as therapeutic targets embedded in the host cell plasma membrane

Lili Zhao<sup>1</sup> | Fuwang Chen<sup>1</sup> | Oliver Quitt<sup>1</sup> | Marvin Festag<sup>1</sup> | Marc Ringelhan<sup>2</sup> | Karin Wisskirchen<sup>1</sup> | Julia Festag<sup>1</sup> | Luidmila Yakovleva<sup>3</sup> | Camille Sureau<sup>4</sup> | Felix Bohne<sup>1</sup> | Michaela Aichler<sup>5</sup> | Volker Bruss<sup>1</sup> | Maxim Shevtsov<sup>3,6</sup> | Maarten van de Klundert<sup>1</sup> | Frank Momburg<sup>7</sup> | Britta S. Möhl<sup>1,8</sup> | Ulrike Protzer<sup>1,8</sup>

<sup>1</sup>Institute of Virology, Technical University of Munich/Helmholtz Zentrum München, TUM School of Medicine, Munich, Germany

<sup>2</sup>Department of Internal Medicine II, University Hospital rechts der Isar, Technical University of Munich, Munich, Germany

<sup>3</sup>Laboratory of Biomedical Nanotechnologies, Institute of Cytology of the Russian Academy of Sciences (RAS), St. Petersburg, Russia

<sup>4</sup>Molecular Virology laboratory, Institut National de la Transfusion Sanguine, Paris, France

<sup>5</sup>Research Unit Analytical Pathology, Helmholtz Zentrum München, Munich, Germany

<sup>6</sup>Center for Translational Cancer Research, University Hospital rechts der Isar, Technical University of Munich, Munich, Germany

<sup>7</sup>Clinical Cooperation Unit Applied Tumor Immunity, German Cancer Research Center, Heidelberg, Germany

<sup>8</sup>German Center for Infection Research (DZIF), Munich Partner Site, Munich, Germany

## Correspondence

Prof. Ulrike Protzer, Institute of Virology,  
Trogerstr. 30, 81675 Munich, Germany.  
Email: protzer@tum.de; protzer@helmholtz-  
muenchen.de

## Funding information

Deutsche Forschungsgemeinschaft, Grant/  
Award Numbers: TRR179 project number  
2378635, TP18; Deutsches Zentrum für  
Infektionsforschung, Grant/Award Number:  
DZIF Academy Maternity Leave Stipends TI  
07.005; Helmholtz-Gemeinschaft, Grant/  
Award Number: Helmholtz Validation Fund;  
Russian Foundation for Basic Research, Grant/  
Award Number: 20-38-70039; Ministry of  
Science and Higher Education of the Russian  
Federation

## Abstract

Hepatitis B virus (HBV) infection is a major health threat causing 880,000 deaths each year. Available therapies control viral replication but do not cure HBV, leaving patients at risk to develop hepatocellular carcinoma. Here, we show that HBV envelope proteins (HBs)—besides their integration into endosomal membranes—become embedded in the plasma membrane where they can be targeted by redirected T-cells. HBs was detected on the surface of HBV-infected cells, in livers of mice replicating HBV and in HBV-induced hepatocellular carcinoma. Staining with HBs-specific recombinant antibody MoMab recognising a conformational epitope indicated that membrane-associated HBs remains correctly folded in HBV-replicating cells in cell culture and in livers of HBV-transgenic mice *in vivo*. MoMab coated onto superparamagnetic iron oxide nanoparticles allowed to detect membrane-associated HBs after HBV infection by electron microscopy in distinct stretches of the hepatocyte plasma membrane. Last but not least, we demonstrate that HBs located on the cell surface allow therapeutic targeting of HBV-positive cells by T-cells either engrafted with a chimeric antigen receptor or redirected by bispecific, T-cell engager antibodies.

Lili Zhao, Fuwang Chen, Oliver Quitt and Marvin Festag contributed equally to this work.

This is an open access article under the terms of the Creative Commons Attribution-NonCommercial-NoDerivs License, which permits use and distribution in any medium, provided the original work is properly cited, the use is non-commercial and no modifications or adaptations are made.

© 2021 The Authors. *Cellular Microbiology* published by John Wiley & Sons Ltd.

### Take Aways

- HBs become translocated to the plasma membrane.
- Novel, recombinant antibody confirmed proper conformation of HBs on the membrane.
- HBs provide an interesting target by T-cell-based, potentially curative therapies.

### KEYWORDS

antiviral therapy, envelope proteins, HBsAg, plasma membrane, T-cell therapy

## 1 | INTRODUCTION

The human hepatitis B virus (HBV) is the prototypical member of the *Hepadnaviridae* family. The virion consists of an icosahedral capsid containing the viral DNA genome. The capsid is enveloped by a cell-derived lipid bilayer carrying the three HBV envelope proteins. Expression of the three isoforms is regulated via transcriptional and translational initiation. The N-terminally extended variants of the small envelope protein (S), referred to as middle (M) and large (L) envelope proteins, share the S protein domain and collectively are referred to as hepatitis B surface (HBs) proteins. Besides infectious virions, an excess of subviral particles (SVPs) is produced and secreted in 1,000- to 100,000-fold excess over virions (Blumberg, 1977). SVP contains densely packed, membrane-embedded HBs but does not contain viral DNA. SVP is released in the form of spheres or filaments from infected cells or cells that have integrated HBV-DNA and can be detected as HBsAg in patient blood. Presumably, HBsAg secreted in excess over virions benefits viral persistence by limiting the development of an effective adaptive immune response.

Worldwide, more than 250 million individuals are chronically infected with HBV. Chronically infected individuals have an increased risk of developing liver fibrosis, cirrhosis and hepatocellular carcinoma (HCC), leading to an estimated 880,000 HBV infection-related deaths per year (World Health Organization, 2017). Available antiviral therapy with nucleos(t)ide analogues suppresses viral replication but does not cure the infection and has limited impact on the development of HCC (Chen, Wang, & Lau, 2017; Debarry, Cornberg, & Manns, 2017; Lobaina & Michel, 2017; World Health Organization, 2017). Therapy with (pegylated) interferon (IFN) alpha is limited by severe side effects. Therapy-induced or spontaneous loss of detectable serum HBsAg, regarded as functional cure, is rare but almost completely leverages the odds of developing end-stage liver disease. Therefore, it is anticipated that a therapy that cures HBV would greatly reduce HBV infection-related morbidity and mortality.

The S domain is common for the three envelope proteins and carries the major hydrophilic determinant including the “a” determinant, an extracellular antigenic loop, which defines the antigenic properties of HBsAg, that is, SVPs and virions, of different HBV genotypes (Norder et al., 2004). Different antibody binding properties in the “a” determinant of different HBV genotypes lead to the definition of

HBV serotypes. The extraordinary conformation of this antigenic determinant is composed of two loops formed by numerous disulfide bonds (Bhatnagar et al., 1982; Brown, Howard, Stewart, Ajdukiewicz, & Whittle, 1984; Dreesman et al., 1982; Mangold, Unckell, Werr, & Streeck, 1995; Qiu, Schroeder, & Bridon, 1996). The L protein carries an N-terminal myristoylation as infectivity determinant and the receptor binding regions for the interaction with heparan sulfate proteoglycans and the bona fide HBV receptor, the bile acid transporter sodium-taurocholate co-transporting peptide (NTCP; Leistner, Gruen-Bernhard, & Glebe, 2008; Ni et al., 2014; Schulze, Gripon, & Urban, 2007; Sureau & Salisse, 2013; Yan et al., 2012).

Assembly and release of infectious virions and SVPs are yet not fully understood. There are strong evidences for budding processes at the endoplasmic reticulum but also at the multivesicular bodies (MVBs). Moreover, it was shown that the MVB-associated endosomal sorting complex required for transport (ESCRT) machinery is involved in the release of infectious particles and filamentous SVPs, whereas spheric SVPs are assembled by budding into the endoplasmic reticulum–Golgi intermediate compartment and released via the secretory pathway (Hoffmann et al., 2013; Jiang, Himmelsbach, Ren, Boller, & Hildt, 2015; Lambert, Doring, & Prange, 2007; Stieler & Prange, 2014; Watanabe et al., 2007). Immunohistochemistry (IHC) analysis of liver tissue sections has revealed that in chronically HBV-infected patients, a significant portion of the HBs produced in infected hepatocytes may localise to the cell membrane (Busachi, Ray, & Desmet, 1978; Chu & Liaw, 1995; Safaie et al., 2016). This suggests that with assembly and release of HBV virions and filaments from MVBs, a proportion of the surface antigens become embedded into the MVB membrane and subsequently, upon fission between the MVB and the cell membrane, ends up in and on the cell membrane. Besides, the HBV envelope proteins are modified in the ER/Golgi network and thus could end up in the cellular membrane.

In the current study, we aim at characterising the intracellular localisation of the HBV envelope proteins in HBV-replicating and HBV-infected hepatoma cells as well as in liver specimens using different HBs-specific antibodies. We found that HBs localises to the plasma membrane of HBV replicating cells in its natural conformation. We developed and characterized the conformation-specific, humanised anti-HBs antibody MoMab and showed that MoMab can detect membrane-associated HBs on HBV-infected hepatocytes by

immunofluorescence staining and transmission electron microscopy (TEM) and in liver tissue of HBV-transgenic mice. Furthermore, we demonstrate that membrane-localised HBs can be targeted by redirected T-cells, thus providing an interesting therapeutic target.

## 2 | RESULTS

### 2.1 | HBs localises to the plasma membrane in vivo

As previous studies indicated that HBs may be localised on the membrane of hepatocytes (Busachi et al., 1978; Chu & Liaw, 1995; Safaie et al., 2016) and membranous staining of HBs on hepatocytes strongly correlated with active viral replication (Chu & Liaw, 1995), we evaluated tissue section obtained from livers of HBV-transgenic mice constitutively replicating HBV from integrated, 1.3-fold overlength HBV genome (Guidotti, Matzke, Schaller, & Chisari, 1995) and from HBV-infected patients who have developed HCC. IHC staining using HBs-specific antibody 70-HG15 revealed that the extent of HBs staining in hepatocytes shows large interindividual variation but also varies from

cell to cell (Figures 1 and S1). Accumulation of HBs on the cell membrane was observed in cells with both high- and low amounts of intracellular HBs in transgenic mice in which each hepatocyte contains the same transcription template (Figure 1a). In liver biopsies from chronic hepatitis B patients, HBs staining was highly variable from cell-to-cell distribution and showed a mixed pattern (Figures 1b and S1), but staining indicative for a membranous localisation was found in the presence or absence of concomitant cytoplasmic staining. Taken together, our IHC results confirmed the speckled membranous localisation of HBs that has been described before in liver tissue.

### 2.2 | Membrane-associated HBs is derived from endogenously expressed protein

To determine whether membranous HBs are derived from endogenously expressed protein translocated to the plasma membrane, we stained HBs by immunofluorescence on HepG2.2.15 and HepAD38 cells, which constitutively replicate HBV. To prevent the detection of intracellular HBs, cells were stained with different anti-HBs antibodies

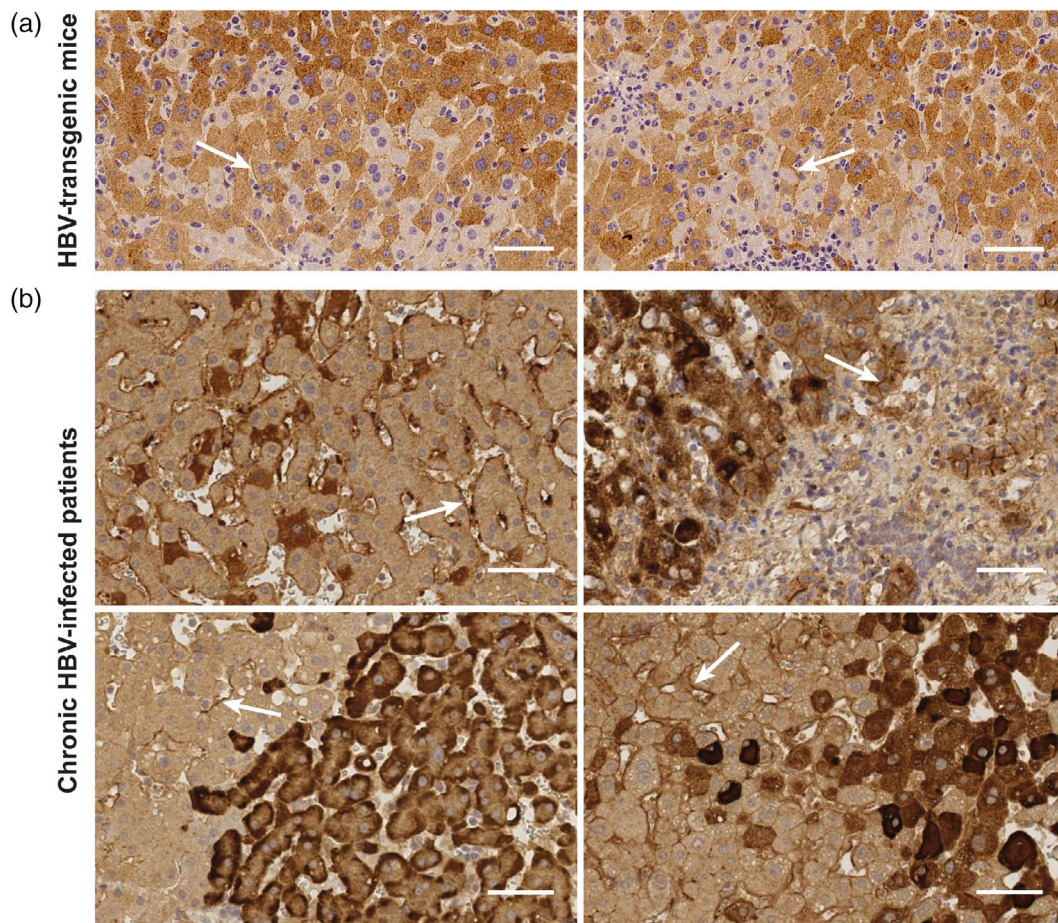


**FIGURE 1** Intrahepatic HBs distribution and localisation in liver sections. Immunohistochemistry staining for HBs to determine distribution in liver tissue of (a) HBV-transgenic mice and (b) hepatocellular carcinoma resected from HBV-infected humans. HBs was stained using the HBs-specific antibody 70-HG15. Membrane-associated HBs is indicated by white arrows. Scale bars represent 50  $\mu$ m. HBs, hepatitis B surface proteins; HBV, Hepatitis B virus

(HBVax, HB01, 5F9) prior to permeabilisation. Co-staining with wheat germ agglutinin (WGA) revealed that HBs localises to the plasma membrane on HepG2.2.15 cells (Figure 2a) as well as HepAD38 cells (data not shown). Membranous HBs distribution was characterized by a distinct punctuate pattern (Figure 2a). When parental HepG2 cells were incubated with supernatant of HepG2.2.15 cells prior to staining with anti-HBs antibody 5F9 to allow binding of secreted SVP to the

cell membrane, we were not able to stain HBs on the cell membrane (Figure 2b). This indicates that the membrane-associated HBs on HepG2.2.15 cells are derived from intracellularly expressed HBs.

Next, Huh-7 cells were transfected with plasmid DNA expressing either the S or L HBV envelope protein or all HBs isoforms combined (SML; Figure 3a). Transfected cells were lysed, and supernatants were collected at 24-, 48- and 72-hr post-transfection. Protein expression

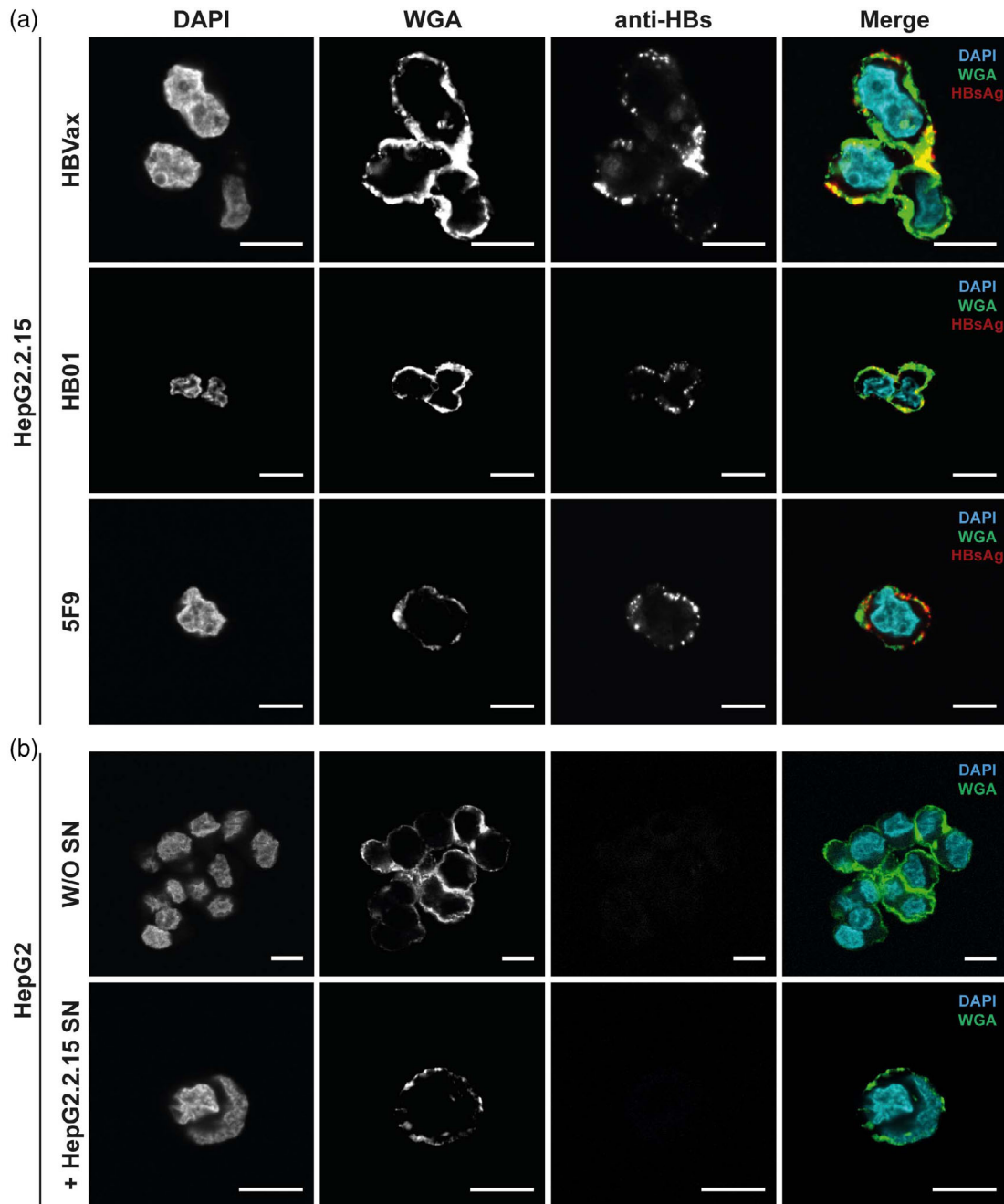


**FIGURE 2** Membrane-associated HBs is derived from endogenously expressed HBs. (a) HepG2.2.15 cells, which constitutively replicate HBV, were incubated with the indicated HBs-specific antibodies before permeabilisation. Confocal microscopic analysis shows that HBs (white, merged images on the right, red) co-localises with the cell membrane, which was stained with wheat germ agglutinin (WGA, green). (b) HepG2 cells were incubated with HepG2.2.15 supernatant (SN) prior to HBs staining with 5F9. Neither staining of HepG2 cell without (W/O SN) nor after incubation with HepG2.2.15 SN detected HBs on the cell membrane. Chromatin was co-stained by DAPI (cyan). Exemplary representative stainings of five independent experiments are shown. Scale bars represent 10 μm. HBs, hepatitis B surface proteins; HBV, Hepatitis B virus; WGA, wheat germ agglutinin

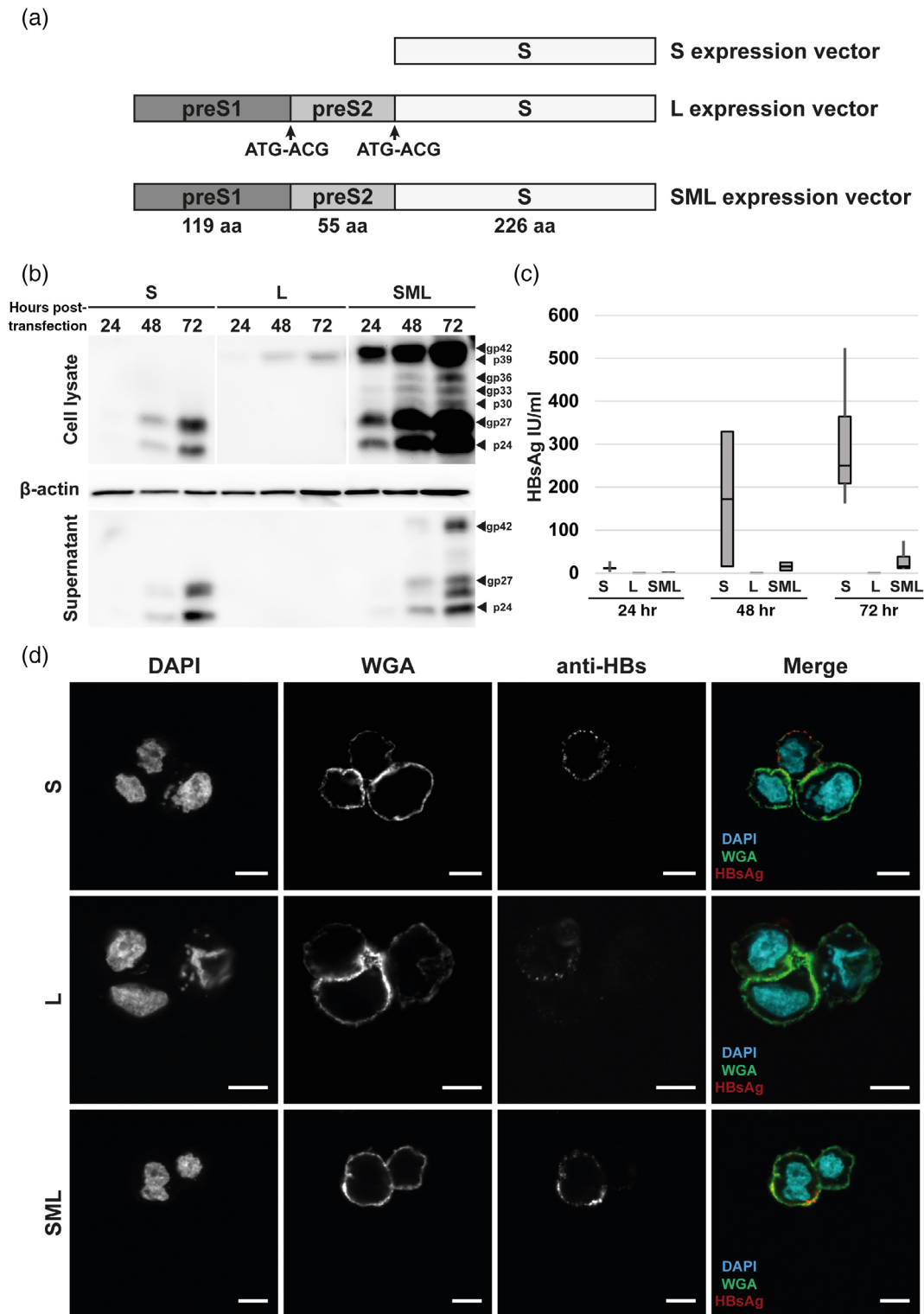


**FIGURE 3** HBs are embedded in the cell membrane independent of SVP secretion. (a) Schematic overview of plasmids expressing only HBV S- or L-protein or all three envelope proteins (SML) of HBV genotype A. To express the L protein in absence of M and S proteins, the respective start codons were mutated (ATG-ACG, indicated by arrows). (b) Western blotting analysis of the cell lysates (upper panel) and supernatants (bottom panel) of transfected Huh-7 cells using a monoclonal, S-specific antibody (HB01). S, M and L proteins were expressed in transfected Huh-7 cells in non-glycosylated and glycosylated forms at 24, 48 and 72 hr post-transfection. Beta-actin was used as a loading control. (c) HBsAg was quantified in the supernatant of transfected Huh-7 cells using the Architect™ HBsAg QT assay. HBs could be detected in the supernatant of cells expressing the S or SML protein(s) but not the L protein alone. Graph represents the average and mean  $\pm$  SD of three independent experiments. (d) Confocal microscopic analysis of non-permeabilised S-, L- or SML-transfected Huh-7 cells confirmed the speckled membrane localisation of HBs (white, merged images: red). The plasma membrane was co-stained using WGA staining (green) and chromatin by DAPI-staining (cyan). Exemplary representative stainings of two independent experiments are shown. Scale bars represent 10  $\mu$ m. HBs, hepatitis B surface proteins; WGA, wheat germ agglutinin

and secretion were confirmed by western blot analysis (Figure 3b). For sensitive detection of secreted HBsAg, the Architect™ HBsAg QT assay was applied (Figure 3c). In line with observations by others, the L protein, when expressed in absence of the S protein, was not secreted (Figure 3b,c). We observed comparable glycosylation of the envelope proteins expressed from the different vectors. Expression levels of L were low when no S and M were co-expressed and L alone was not secreted (Figure 3b), as shown before (Chisari et al., 1987; Roingeard & Sureau, 1998). Immunofluorescent staining of non-permeabilised Huh-7 cells transfected with the S-, L- and SML-expressing plasmid vectors revealed that in all cells, HBs is associated with the plasma membrane in a distinct, punctuate pattern. Exemplary staining using the HBs-specific antibody HB01 is shown (Figure 3d). The observation that L, although it cannot be

secreted in SVP on its own, locates to the plasma membrane confirms that HBs detected on the cell surfaces are derived from endogenously expressed HBs. To further prove that L locates to the plasma membrane, we performed a surface immunoprecipitation with L- and mCherry-L-transfected Huh-7 cells incubated with the specific anti-HBs antibodies 5F9 and 20HR20 prior lysis and precipitation. Localisation of L in the plasma membrane was confirmed by western blot analysis. To verify proper processing of L alone as shown before (Kluge, Schlager, Pairan, & Bruss, 2005), we treated cell lysates with peptide: N-glycosidase F (PNGaseF) and analysed the glycosylation pattern using western blotting (Figure 4a). L was fully deglycosylated by PNGaseF (Figure 4a) verifying the proper processing of L alone. A comparison of the cellular localisation of L with mCherry-L showed that the level of L (Figure 4b) localised to

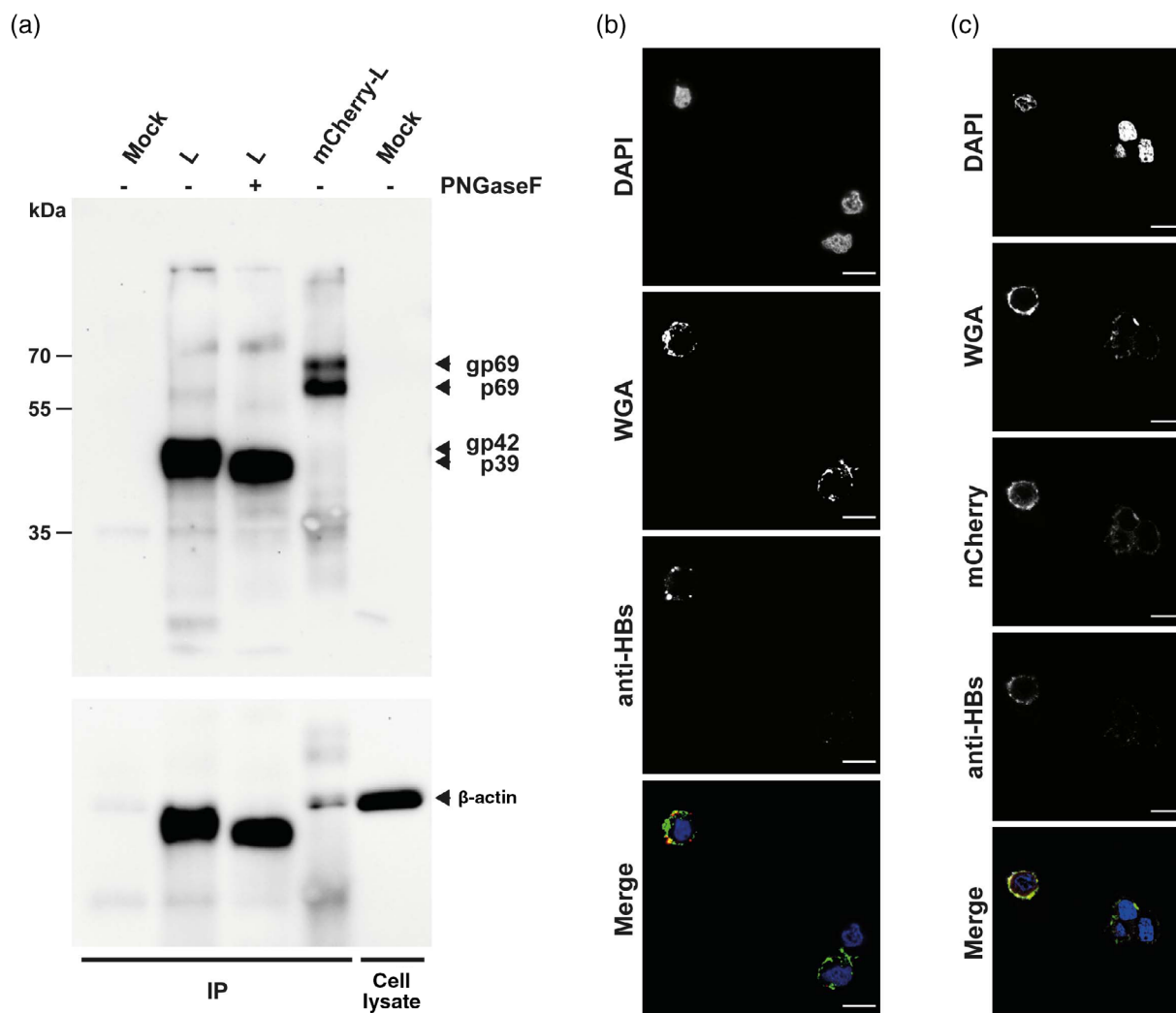


**FIGURE 4** HBs are embedded in the Huh-7 cell membrane. (a) Western blotting analysis of the surface IP samples and cell lysate (right lane) of transfected Huh-7 cells using a monoclonal, S-specific antibody (HB01). L proteins were expressed in transfected Huh-7 cells and deglycosylated by PNGaseF treatment. Beta-actin was used as a control of successful IP. (b) Huh-7 cells were transfected with a plasmid-expressing L protein. Cells were stained with anti-preS1 antibody 20HR20, followed by Alexa-Fluor® 647 fluorochrome (white, merged images: red) before fixation and permeabilisation. (c) Huh-7 cells were transfected with a plasmid expressing a mCherry-L fusion protein (red). The cell membrane was co-stained with WGA (green), and cell nuclei were stained with DAPI (Blue). Scale bars represent 2  $\mu$ m. HBs, hepatitis B surface proteins; WGA, wheat germ agglutinin

the plasma membrane was low when compared to mCherry-L (Figure 4c) localisation in the cytoplasm.

### 2.3 | Characterisation of the new humanised HBs-specific antibody MoMab

To characterize membrane-associated HBs in detail, we constructed a chimeric, human antibody designated as MoMab. MoMab is a homodimer of a human single-chain antibody fragment (scFv C8; Bohne et al., 2008) directed against the S domain of all three HBV envelope proteins that have been terminally fused to the constant region (CH2 and CH3) of human IgG1 (Figure 5a). The scFv C8 originates from an scFv library that was derived from peripheral blood lymphocytes of individuals vaccinated against hepatitis B and was selected because of its high affinity to HBs-expressing hepatoma cells. MoMab was expressed in HEK 293 cells and purified from cell culture supernatant by ion exchange chromatography. Coomassie blue staining of purified MoMab separated by polyacrylamide gel electrophoresis under reducing and non-reducing conditions indicated that the purified MoMab was free of other protein contaminations (Figure S2a). As surface plasmon resonance did not allow us to determine an “off”-rate, neither using MoMab nor purified scFv (data not shown), we decided to determine the binding affinity using an ELISA with patient-derived HBsAg (genotype adw) that was free of any anti-HBs. This method revealed a EC50 of purified MoMab that contains two HBs-binding domains (Figure S2a) to immobilised HBsAg of 0.64 nM (Figure 5b).

Next, we determined the epitope within the S-protein domain targeted by MoMab using an alanine-scanning approach. Point mutants of S within its “a” determinant (aa 101–225) were expressed in mammalian cells, immobilised and exploited to assess MoMab binding (Figure S2b). Residues that, when mutated, disrupted the interaction between MoMab and HBs were mapped onto the hypothetical structure of the S protein (van Hemert et al., 2008), revealing that MoMab targets the antigenic loop of the “a” determinant (Figures 5c and S2b). The largest impacts on MoMab binding to HBs were monitored for the major immune-dominant residues such as the charged residues K141 and D144 as well as the non-charged, polar residue T148 within the antigenic loop (Figures 5c and S2b). Interestingly Y225, which is highly conserved among all HBV genotypes except genotype F, was also an important residue determining the conformational epitope recognised by MoMab (Figures 5c and S2b). ELISA analysis using the antibody on immobilised HBsAg indicates that MoMab recognises HBsAg from different serotypes and divergent origins such as yeast, Chinese hamster ovary cells and human serum (Figure 5d). However, MoMab did not recognise HBsAg (Figure 5d), which is known to have lost its native structure. All these results highlight that MoMab binding is highly confirmation dependent.

To show that the relatively low amounts of HBs ending up on the cell surface suffice to bind the MoMab, we stained HepG2 cells transfected with a plasmid expressing a mCherry-S fusion protein as well as HBV-infected HepG2-NTCP cells. As the cells were not permeabilised, the abundant HBs accumulating in ER membranes could

not be targeted by the MoMab added. Purified MoMab specifically interacted with HBs on the surface of mCherry-expressing HepG2 cells but not with neighbouring HBs-negative cells (Figures 5e and S2c) and with HBV-infected HepG2-NTCP cells (Figures 5f and S2d). Staining intensity increased with the MOI used for infection of HepG2-NTCP cells (Figure S3). To assess whether MoMab has neutralising activity, purified HBV was pre-incubated with different concentrations of MoMab (1 µg, 0.1 µg and 0.01 µg) before the infection of HepG2-NTCP cells. Pre-incubation with MoMab dose dependently inhibited HBV infection as shown by a decrease of HBeAg and HBsAg secretion 4, 8 and 12 days postinfection (dpi) as well as intracellular HBV pregenomic RNA and cccDNA determined 12 dpi (Figure 6).

Taken together, these data show that the chimeric, recombinant human MoMab antibody detects a conformational epitope within the “a” determinant of the S domain of HBV envelope proteins of different serotypes with high avidity and is able to neutralise HBV infection. It sensitively detects HBs on the surface of HBs-expressing and HBV-infected cells.

### 2.4 | Detection of HBs by MoMab-conjugated nanoparticles

To visualise membrane-associated HBs on the cell surface and exclude detection of HBV particles bound to the cell surface, MoMab was conjugated to dextran-coated superparamagnetic iron oxide nanoparticles (SPIONs) allowing detection by TEM. A “switch” assay of MoMab-conjugated SPIONs co-incubated with soluble HBsAg demonstrated correct formation of antibody conjugates by an increase in the T2 relaxation time (Figure S4). MoMab-conjugated SPIONs were incubated with constitutively HBV-replicating cells (HepG2.2.15 and HepAD38) and HBV-infected HepG2-NTCP cells. EM analysis demonstrated that MoMab-SPIONs bind the plasma membrane of all HBV-replicating cells (Figure 7). In accordance with the punctuate in immunofluorescence stainings we observed (Figure 5e,f), HBs was concentrated at certain membrane areas. There was little indication for binding to viral or sub-viral particles. HBs visualised by MoMab-SPION binding was distributed at certain membrane stretches on cell protrusions where they tend to cluster.

### 2.5 | HBs on the cell surface allows therapeutic targeting by CAR-T cells or T-cell engager antibodies

To assess whether the MoMab would target membrane-associated HBs in vivo, Alb-Psx transgenic mice that express HBV L protein under control of an albumin promoter in hepatocytes were intravenously injected with 100 µg MoMab. Because mainly L protein but little S protein is expressed, these mice have low or even no detectable HBsAg levels in their blood. Four hours after MoMab injection, HBsAg level in serum and intrahepatic HBs was quantified. In one mouse with detectable HBsAg level, serum HBsAg decreased from 43.35 IU/ml to

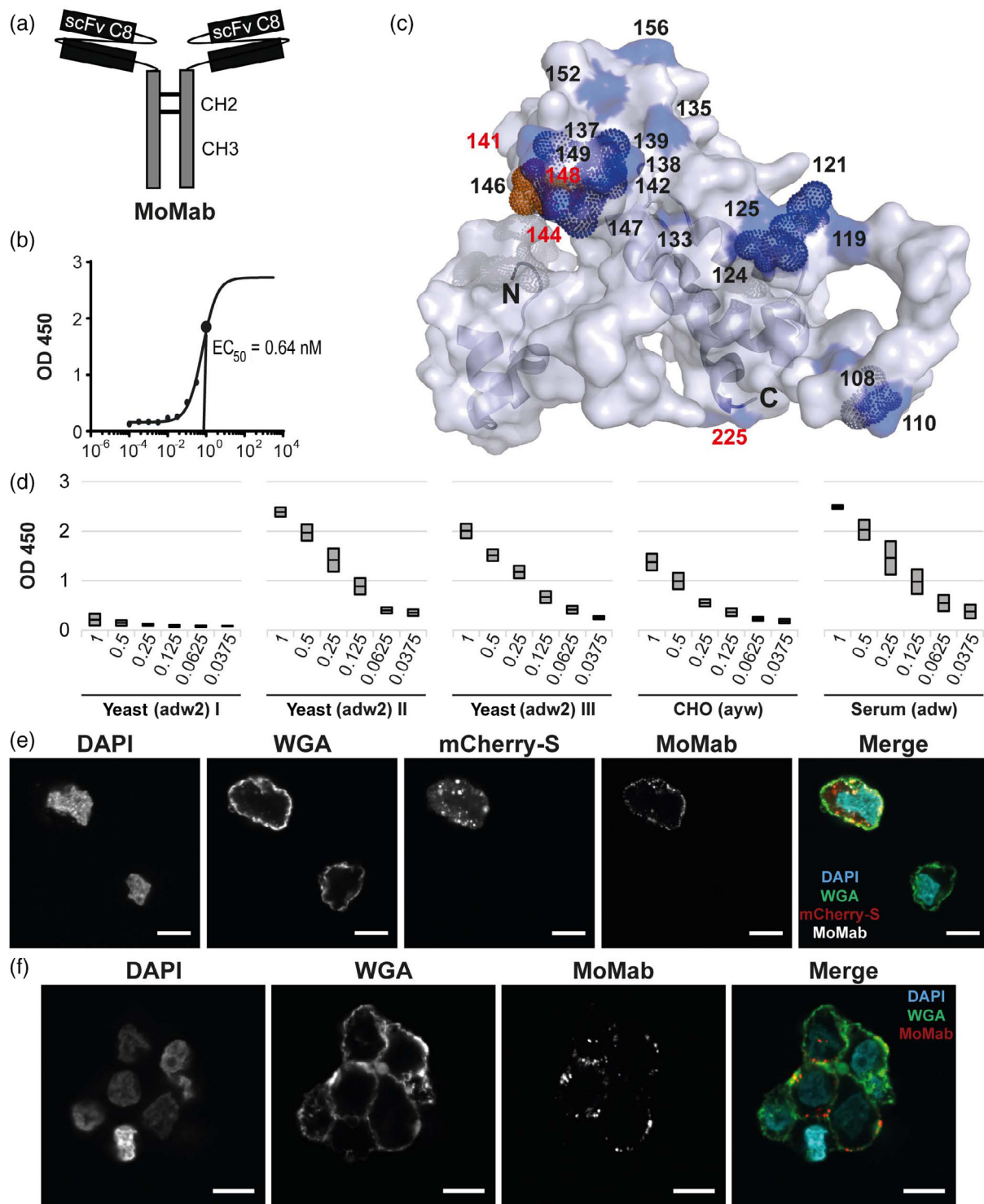


**FIGURE 5** Generation and characterisation of a human, recombinant antibody for detection of HBVs. (a) Schematic representation of the recombinant human antibody MoMab. A human single-chain antibody fragment (scFv C8) was N-terminally fused to the constant region (CH2 and CH3) of human IgG1 heavy chain replacing VH and CH1 domains. (b) The avidity of MoMab for immobilised HBsAg purified from patients' serum was determined by ELISA, revealing an EC<sub>50</sub> of 0.64 nM. (c) HBs residues that are involved in the interaction between MoMab and HBs were identified by an alanine scanning analysis (see Figure S2b) and mapped to a theoretical model of the HBV S structure (pdb file modified from van Hemert, Zaaijer, Berkhout, & Lukashov, 2008). Amino acids of S that are part of the MoMab epitope are shown in blue. Numbers indicate amino acid positions, numbers in red indicate residues most critical for the interaction. Cystein mutations that disrupted the interaction between MoMab and HBs and the glycosylation site N146 (orange) are shown as dotted spheres. The N- and C-terminus are indicated with N and C, respectively. (d) HBsAg from different serotypes and divergent origins (yeast, CHO cells and serum) was immobilised on ELISA plates at different concentrations. The capacity of MoMab to interact with immobilised antigen was determined by ELISA. Graph represents the average and mean  $\pm$  SD of two experiments performed in triplicate. (e) HepG2 cells were transfected with a plasmid expressing a mCherry-S fusion protein (red). (f) HepG2-NTCP cells were infected with HBV at MOI 500. Cells were stained with MoMab coupled to Alexa-Fluor<sup>®</sup> 647 fluorochrome (white) before fixation and permeabilisation. The cell membrane was co-stained with WGA (green), and cell nuclei were stained with DAPI (Blue). Representative pictures obtained in two independent experiments are shown. Scale bars represent 10  $\mu$ m. WGA, wheat germ agglutinin

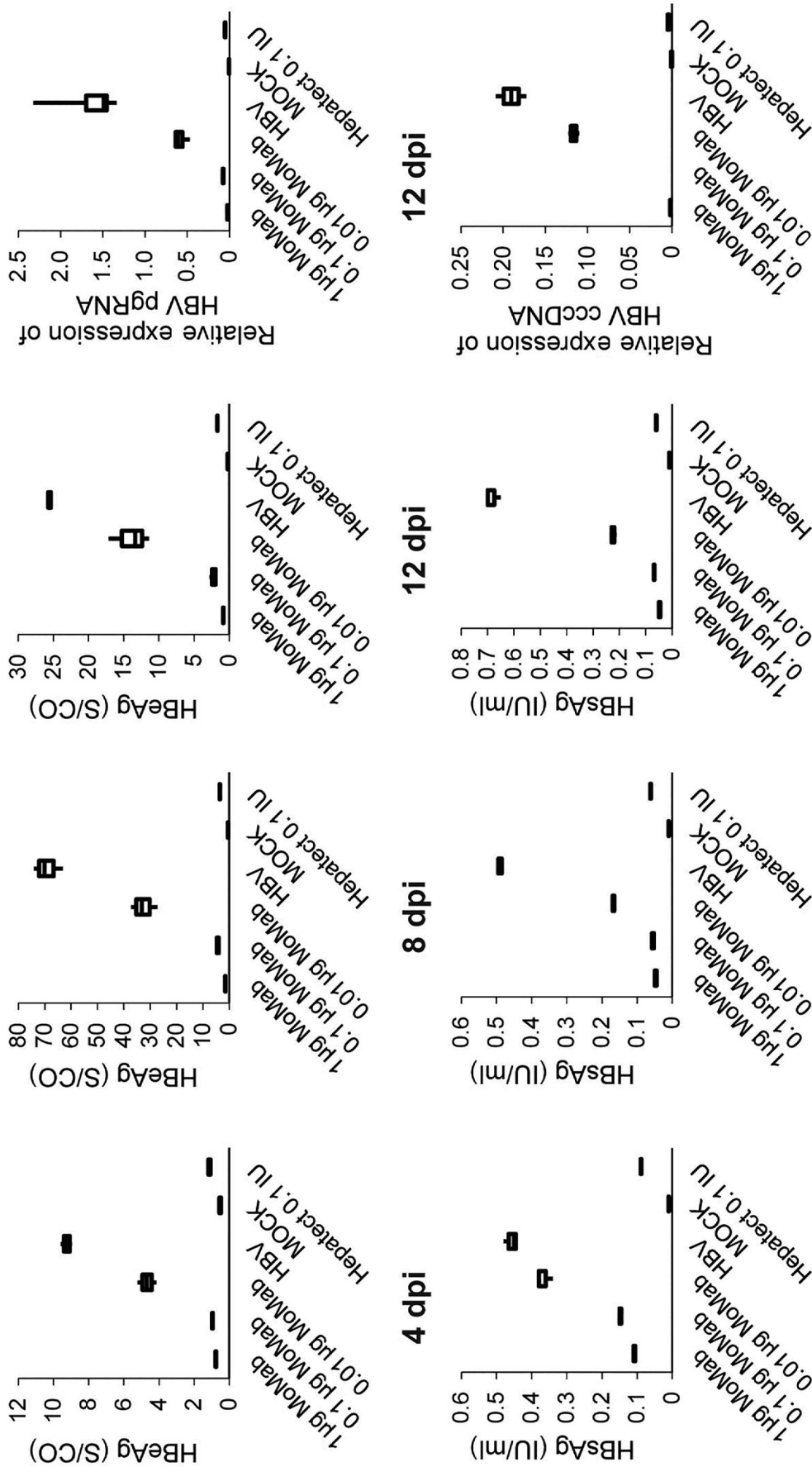


**FIGURE 6** Characterisation of a neutralising human, recombinant antibody for detection of HBs. For the neutralisation assay, purified HBV was incubated with different amounts of MoMab and applied to infect HepG2-NTCP K7 cells at MOI 100. HBsAg and HBsAg levels were determined in cell culture supernatant collected from Day 4, 8 and 12 postinfection and are given as signal over cut-off (S/CO) and international units (IU) per ml, respectively. Cells were lysed 12 dpi, and intracellular HBV pregenomic RNA (pgRNA) and cccDNA were determined by qPCR. Relative expression levels after normalisation to housekeeping gene  $\beta$ -actin are shown. Graphs represent the mean  $\pm$  SD of triplicate infection experiments. HBV, Hepatitis B virus

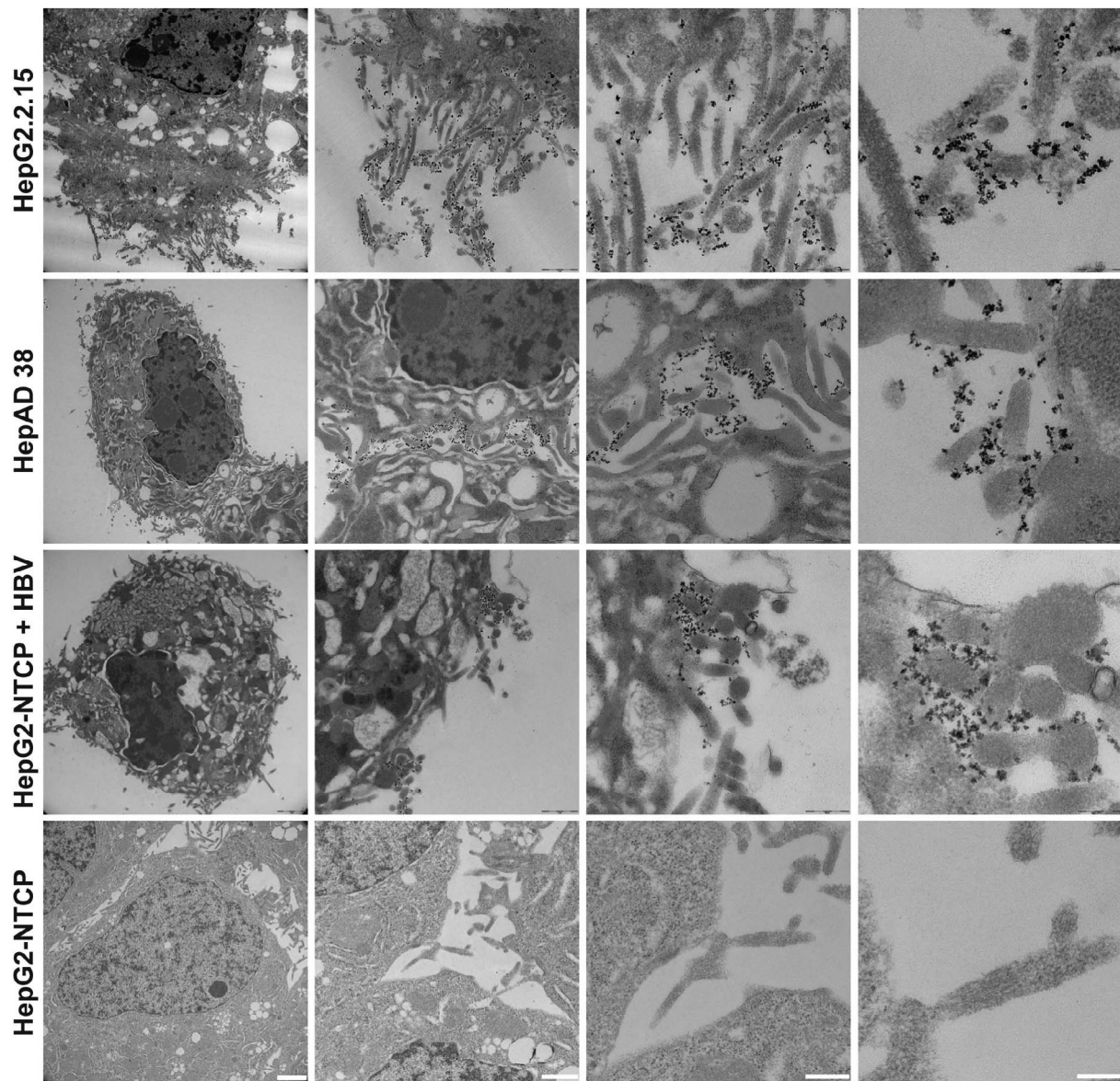


**FIGURE 7** MoMab-coupled iron particles indicate localisation of HBs to distinct membrane stretches on the hepatocyte surface. MoMab was coupled to SPIONs and incubated on HepG2.2.15 (top row) or HepAD38 cells (second row) constitutively replicating HBV, HBV-infected HepG2-NTCP cells (third row) and non-infected control cells (fourth row). After fixation, TEM of ultrathin sections was performed. Cells visualised by EM at increasing magnification (from left to right) showed binding of MoMab-SPIONs localising to the membranes on protrusions of HBV replicating but not of HBV-negative HepG2-NTCP cells. Scale bars (white) from the left to the right indicate 2  $\mu$ m, 1  $\mu$ m, 500 nm and 200 nm. HBV, Hepatitis B virus; NTCP, sodium-taurocholate co-transporting peptide

8.95 IU/ml after MoMab injection (data not shown). In this mouse, MoMab was detected in the liver by staining with an anti-human antibody, indicating that MoMab-targeted HBs expressed on hepatocytes *in vivo* (Figure 8a). MoMab did not target hepatocytes of wild-type C57BL/6 mice (Figure 8b).

To therapeutically target HBs on HBV-infected cells, T-cells can be redirected using a chimeric antigen receptor (CAR; Bohne et al., 2008) or T-cell engager antibodies that contain the scFv C8 antibody targeting HBs and either a CD3 or a CD28 scFv activating T-cells (BiMab; Quitt et al., 2021). Huh-7 cells transfected with plasmid expressing S, L or SML proteins served as target cells.

Human T-cells were engrafted with an scFv C8-based CAR (S-CAR; Bohne et al., 2008) by retroviral transduction. In line with earlier experiments (Krebs et al., 2013), viability analysis revealed that engrafted T-cells specifically killed Huh-7 cells expressing the HBV S-protein or all three envelope proteins (SML; Figure 8c). The same was observed when T-cells from healthy donors were redirected and specifically activated by the BiMab (Figure 8d). S-CAR T-cells as well as BiMab activated T-cells, however, also killed Huh-7 cells only expressing L protein preventing that T-cells can be activated by viral particles or SVP secreted (Figure 3c) and ensuring that only HBs located to the plasma membrane can be targeted (Figure 8c,d).

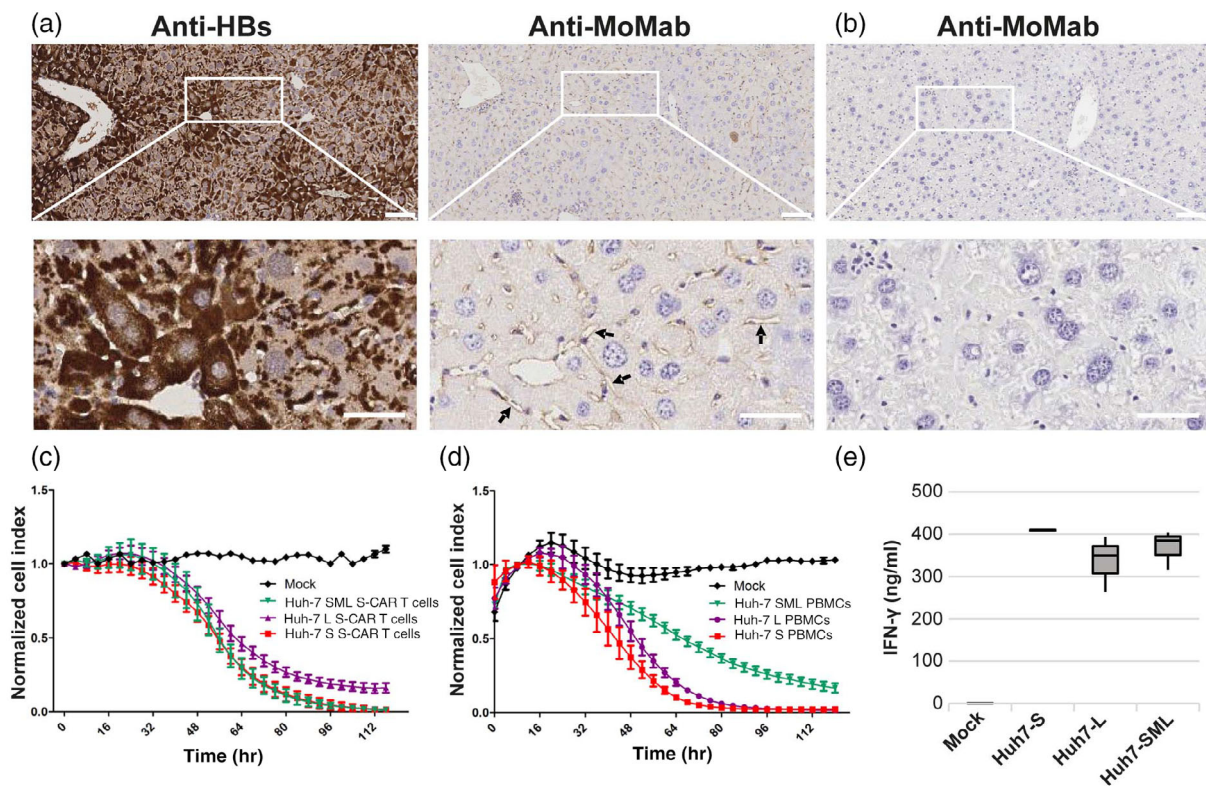


**FIGURE 8** Targeting of membrane-localised HBs by antibodies and CAR-T cells. (a) 100  $\mu$ g purified MoMab were iv injected into four AlbPxs mice that expresses HBV L protein. After 4 hr, mice were sacrificed and livers collected. HBs was stained using anti-HBs antibody 70-HG15 or an anti-human antibody to detect the MoMab that had been injected. (b) MoMab-staining of liver sections of WT-mice served as negative control. Scale bars represent 50  $\mu$ m. (c-d) Huh-7 cells were transfected with plasmid DNA to express only HBV S- or L-protein or all three envelope proteins (SML). (c) Transfected cells were co-cultured with human T-cells engrafted with a scFv C8-based chimeric antigen receptor (S-CAR). Cell viability was followed by real-time cytotoxicity analysis for 4 days using an xCelligence device. Normalised cell index indicated that the engrafted T-cells specifically killed all HBs-expressing Huh-7 cells. (d) Transfected Huh-7 cells were co-cultured with human PBMCs in the presence of a bispecific T-cell engager antibody. Cell viability was followed on the xCelligence device for 4 days, indicating that the redirected T-cells specifically killed all HBs-expressing Huh-7 cells. (e) Evaluation of IFN- $\gamma$  in the supernatant of PBMCs co-cultured with HBs-expressing Huh-7 cells by ELISA. HBs, hepatitis B surface proteins; IFN, interferon; PBMC, peripheral blood mononuclear cell

Determining IFN- $\gamma$  in cell culture supernatant showed that S-CAR T-cells were specifically activated in co-culture experiments (data not shown), but also T-cells were activated by T-cell engager BiMab upon binding to HBs on the target cell surface (Figure 8e). Both therapeutic approaches proved that HBV S, M and L are expressed on the surface of target cells and can be used to specifically target and kill HBs-expressing or HBV-replicating cells.

### 3 | DISCUSSION

In this study, we could confirm the membranous distribution of HBs in vivo in HBV-transgenic mice and in liver and cancer tissue from chronic hepatitis B patients. Our data verified the membranous distribution in cell culture experiments revealing that HBs shows a speckled membrane localisation in non-permeabilised, HBs-expressing cells. Using a recombinant anti-HBs antibody, MoMab, we confirmed correct conformation of membrane-associated HBs and intravenously injected MoMab localised to hepatocytes in the liver of Alb-Psx

transgenic mice expressing HBs. By EM detecting membrane localisation of HBs in HBV-replicating hepatoma cells and in HBV-infected cells, we establish that membrane-associated HBs is derived from intracellularly expressed HBs and does not result from the attachment of SVPs or virions. T-cells grafted with a CAR using the same scFv as the MoMab specifically eliminated Huh-7 cells expressing HBV L-protein that is not secreted excluding the possibility that SVP or virions binding back to the cell membrane after secretion are targeted. Taken together, our study demonstrates that membrane-associated HBs enable the development of new and promising approaches to detect, monitor and treat HBV infection.

In this study, we characterized the membrane-localisation of HBs in vivo staining hepatocytes from liver specimens of HBV-transgenic mice and chronically infected patients. Our results confirm a previous report performing indirect immunofluorescence on liver specimens. In tissue sections from 75 patients with chronic hepatitis B, the authors found purely membranous or solely cytoplasmic as well as mixed staining of HBs on hepatocytes (Chu & Liaw, 1995). Moreover, this study indicated that the distinct membranous pattern of HBs is a

sensitive and specific marker of active replication (Chu & Liaw, 1995). It is well known that there is a correlation between hepatocarcinogenesis and high HBsAg levels in patients (Chisari et al., 1989; Sunami et al., 2016). Dependent on the presence of HBeAg, HBs distribution seems to be different. The majority of the HBeAg-negative cases had a “patchy” or membranous HBsAg distribution compared to only 50% among HBeAg-positive cases (Chu & Liaw, 1995; Safaie et al., 2016).

The punctate membrane-located HBs staining by IHC (Chu & Liaw, 1995; Safaie et al., 2016) needed to be verified in non-permeabilised hepatocytes with an intact plasma membrane. Therefore, an indirect immunofluorescence protocol with antibody staining before fixing the cells was established. By this approach, we confirmed a speckled membrane distribution of HBs in HBV-replicating cells but could neither detect this in non-infected HepG2 cells nor in HepG2 cells pre-incubated with HBV virions. The speckled HBs-localisation within the plasma membrane was confirmed by different HBs-specific antibodies such as HB01 and 5F9, which both recognise a linear epitope within the “a” determinant of S as reported before (Berkower et al., 2011; Inoue et al., 2015). Using transiently transfected Huh-7 cells expressing L but no S protein, we verified the punctate membrane localisation of HBs independently of SVP secretion and circulating virions that may be adsorbed (Chisari et al., 1987; Roingard & Sureau, 1998). Moreover, we could proof the proper processing and membrane localisation of L using surface IP.

In previous studies, we have shown that T-cells grafted with scFv C8 can specifically target cells infected with HBV or replicating HBV (Bohne et al., 2008; Krebs et al., 2013). To visualise and demonstrate localisation of HBs to the plasma membrane, we constructed a new recombinant, human antibody that we named MoMab, containing two C8 binders attached to the constant region (CH2 and CH3) of human IgG1 based on this scFv. MoMab recognises a conformational epitope within the “a” determinant of S verified using constitutive mutants of the AGL region and has the capability to neutralise HBV infection. Staining with MoMab confirmed the speckled, membranous distribution of HBs on HBV-replicating and HBV-infected cells by immunofluorescence microscopy and by EM. Using S-CAR-grafted T-cells, we demonstrated that not only cells expressing S or co-expressing all three envelope proteins are targeted but also cells that express only L protein. Furthermore, we found that intravenously injected MoMab could target hepatocytes in the liver of Alb-PSX mice expressing the HBV L protein (Chisari et al., 1989). HBV L protein, when expressed alone, is not secreted (Chisari et al., 1987; Roingard & Sureau, 1998). We demonstrate that L protein, when expressed in absence of the other HBs proteins, can still be targeted on the hepatocyte membrane of transfected cells and transgenic animals, indicating that the localisation of HBs on the membrane is independent of SVP or virion secretion. These data strongly support the hypothesis that HBs can be transported via MVBs that finally bud in the plasma membrane and transport the HBV envelope proteins to the cell membrane.

The endosomal sorting pathway via the formation of MVBs drives the release of infectious virions and filaments (Hoffmann et al., 2013;

Jiang et al., 2015; Lambert et al., 2007; Stieler & Prange, 2014; Watanabe et al., 2007), whereas spheric SVPs are released by the constitutive secretion pathway (Huovila, Eder, & Fuller, 1992). Secretion of proteins via the endosomal sorting pathway is mediated by the ESCRT (consisting of ESCRT-0, ESCRT-I, ESCRT-II and ESCRT-III). It was described before that L protein—like the Gag protein of HIV—is linked to the ESCRT-I component tsg 101 via alpha-taxilin (Hoffmann et al., 2013) and gamma 2-adaptin (Lambert et al., 2007) implying that L protein is involved in recruiting the ESCRT machinery and activating the ESCRT-MVB secretion pathway. These interactions could induce MVB plasma membrane fission at the budding site and thereby facilitate HBV release (Blumberg, 1977; Hoffmann et al., 2013; Huovila et al., 1992; Jiang et al., 2015; Lambert et al., 2007; Stieler & Prange, 2014; Watanabe et al., 2007). Interestingly, the assembly and release of SVPs derived from S alone occur ESCRT-MVB-independent (Lambert et al., 2007). The mechanism of how HBs is involved in the ESCRT-MVB-driven exit of HBV is the major question of intense studies. It is still elusive how HBs is incorporated in MVB and thereby involved in the release of infectious virions and filaments from the infected hepatocyte.

In summary, we show that HBs—besides its intracellular localisation and secretion as spheric SVP—localises to the plasma membrane of HBV-infected cells where it is detected by antibodies recognising linear as well as conformational epitopes and can be targeted by redirected T-cells. Translocation to the plasma membrane most likely occurs via MVBs, but further studies are required to validate this hypothesis.

## 4 | EXPERIMENTAL PROCEDURES

### 4.1 | Cell culture

The human hepatoma cell lines Huh-7 (JCRB0403; Nakabayashi et al., 1982), HepG2 (ATCC Cat# HB-8065), HepG2.2.15 (Sells, Chen, & Acs, 1987) and HepG2-NTCP-K7 (Ko et al., 2018) were grown in supplemented Dulbecco's modified Eagle' medium (DMEM) at 37°C in 5% carbon dioxide. DMEM was supplemented with 10% fetal calf serum (FCS), 2 mM L-glutamine, 1% NEM non-essential amino acids, 1% sodium pyruvate, 50 U/ml penicillin/streptomycin (all from Gibco, Thermo Fisher Scientific, Carlsbad, California). HBV-producing HepAD38 cells, kindly provided by Dr. Chris Seeger, were maintained in DMEM/F12 medium supplemented with 10% FCS, 1% penicillin/streptomycin/tetracycline and 0.4% G418 (all from Gibco, Thermo Fisher Scientific, Carlsbad, California) at 37°C in 5% carbon dioxide.

### 4.2 | Human bio-samples and mouse lines used

Mice transgenic for LHBs (Alb-Psx) or a 1.3-fold overlength HBV genome (HBV1.3.3.2) were bred in specific pathogen-free animal facilities and were bred and received human care according to the German Law for the Protection of Animals with permission of the regulatory authority.

Human liver samples were obtained from liver parts directly after resection of HCCs from patients chronically infected with HBV. They were banked in a professional biobank after fixation with 10% neutral-buffered formalin and paraffin embedding fulfilling Tier1 criteria of the Biospecimen Reporting for Improved Study Quality reporting guidelines. Samples were collected and processed with permission of the regulatory authority, authorised by the ethics committee of the University Hospital rechts der Isar of the Technical University of Munich (ref: 5846/13).

### 4.3 | IHC staining

For HBs-staining, liver specimens of HBV-transgenic mice (strain HBV1.3.3.2) (Guidotti et al., 1996) and chronic hepatitis patients who had developed HCC were fixed in 4% paraformaldehyde (PFA) for 24 hr before paraffin embedding; 2- $\mu$ m tissue sections were collected and stained by IHC. To analyse the location of HBs, sections were stained with polyclonal anti-HBs antibodies such as 70-HG15 (goat; Fitzgerald, Acton, Massachusetts) and MoMab (human) and accordingly secondary antibodies were coupled to horseradish peroxidase (Thermo Fisher Scientific, Carlsbad, California). Histological analysis of the 2- $\mu$ m paraffin-embedded tissue sections was performed with the Bond Polymer Refine Detection Kit (Leica, Wetzlar, Germany) on a BondMax system (Leica). Images of the HBs and MoMab stainings were documented by scanning the whole slides using an SCN-400 slide scanner (Leica) and analysed using Tissue IA image analysis software (Leica) with optimised quantification algorithms.

### 4.4 | Fluorescence analysis

To analyse the intracellular HBs distribution, transiently transfected Huh-7 and HBV-positive HepG2.2.15 and Hep-AD38 cells were analysed by confocal microscopy. Huh-7 or HepG2-NTCP cells were transfected with plasmids pSVB45H (expressing SML), pSVL (coding L only) or pSVBX24H (coding S; Siegler & Bruss, 2013), mCherry-L or mCherry-S (expressing S fused to mCherry; Bayer, Banning, Bruss, Wiltzer-Bach, & Schindler, 2016), kindly provided by Volker Bruss, using FuGENE<sup>®</sup> HD transfection reagent (Promega, Madison, Wisconsin) for 48 hr at 37°C. In addition, HBV-infected HepG2-NTCP and HepG2.2.15 cells were stained by indirect immunofluorescence to analyse the cellular location of HBs during viral replication. Parental HepG2 cells served as negative control. To detect HBs, cells were stained with anti-HBs antibodies HBVax (goat, dilution 1:500), HB01 (mouse, 1:200; kindly provided by Prof. Dr. Glebe, University of Gießen, Germany), 5F9 (mouse, 1:200; Golsaz-Shirazi et al., 2016), 20HR20 (rabbit, 1:150; Fitzgerald) and MoMab (human, 1:150) for 1 hr at 4°C and respective secondary Alexa-Fluor<sup>®</sup> 647- or Alexa-Fluor<sup>®</sup> 568-conjugated antibodies (dilution 1:500; Thermo Fisher Scientific, Carlsbad, California) for 45 min at 4°C. The samples were counterstained with the plasma membrane marker WGA coupled to

Alexa-Fluor 488 (Thermo Fisher Scientific) diluted 1:500 for 30 min on ice. As WGA is known to induce chromatin condensation, nuclear fragmentation and DNA release may result in deformed nuclei as observed here (Schwarz, Wojciechowicz, Picon, Schwarz, & Paty, 1999). After washing the samples three times with 1% BSA in PBS, fixation was performed with 4% paraformaldehyde for 10 min at room temperature (RT). For nuclear staining, coverslips were overlaid with DAPI Fluoromount-G<sup>®</sup> Mounting media (Southern Biotech, Birmingham, Alabama). Images were documented by a confocal laser scanning microscope (Fluoview FV10i, Olympus, Hamburg, Germany) and analysed using Image J (Schneider, Rasband, & Eliceiri, 2012) and Photoshop 7.0 (Adobe Software Palo Alto, California).

### 4.5 | Western blot analysis

Huh-7 cells were transfected with plasmids mCherry-L or pSVB45H, pSVL or pSVBX24H (Siegler & Bruss, 2013) using FuGENE<sup>®</sup> HD in OptiMEM<sup>™</sup> reduced serum medium (Thermo Fisher Scientific, Carlsbad, California). Proteins from the whole cell lysates obtained after 24, 48 and 72 hr were separated by sodium dodecyl sulfate-polyacrylamide gel electrophoresis (SDS-PAGE) and stained using the mouse monoclonal S-specific antibody HB01 (1:1000 dilution) overnight at 4°C as described before (Untergasser et al., 2006). For loading control, the blot was incubated with a rabbit antiserum against  $\beta$ -actin (1:10000 dilution; 42 kDa, Sigma-Aldrich, Taufkirchen, Germany) for 1 hr at RT. Then, peroxidase-conjugated goat anti-mouse/anti-rabbit IgG antibodies (Sigma-Aldrich, Taufkirchen, Germany) were used at a dilution of 1:5000 and incubated for 2 hr at RT, followed by the enhanced chemiluminescence detection kit (Amersham Biosciences, Bath, UK).

### 4.6 | Surface immunoprecipitation

Huh-7 cells were transfected with plasmids mCherry-L or pSVL (Siegler & Bruss, 2013) using FuGENE<sup>®</sup> HD in OptiMEM<sup>™</sup> reduced serum medium (Thermo Fisher Scientific, Carlsbad, California). Huh-7 cells were incubated with anti-HBs antibodies 5F9 and 20HR20, lysed and precipitated with IgG beads (Thermo Fisher Scientific, Carlsbad, California). Cell lysates from Huh-7-L expressing cells were treated with PNGaseF (New England Biolabs, Ipswich, Massachusetts) analysing the glycosylation pattern. The samples were separated by SDS-PAGE and stained using the mouse monoclonal S-specific antibody HB01 (1:1000 dilution) overnight at 4°C as described before (Untergasser et al., 2006). For loading control, the blot was incubated with a rabbit antiserum against  $\beta$ -actin (1:10000 dilution; 42 kDa, Sigma-Aldrich, Taufkirchen, Germany) for 1 hr at RT. Then, peroxidase-conjugated goat anti-mouse/anti-rabbit IgG antibodies (Sigma-Aldrich, Taufkirchen, Germany) were used at a dilution of 1:5000 and incubated for 2 hr at RT, followed by the enhanced chemiluminescence detection kit (Amersham Biosciences, Bath, UK).

#### 4.7 | HBV infection and immunoassays

The supernatants of the transfected Huh-7 cells were harvested after 24, 48 and 72 at 37°C. HepG2-NTCP cells (seeded  $5 \times 10^4$ /24-well plate) were differentiated with DMEM containing 1.8% DMSO for 2 days before infection with purified HBV at MOI of 200, 500 or 1,000 virions by adding 4% polyethylenglycol over night as described (Ko et al., 2018). Media was exchanged every 3 days until the end of the experiment. At indicated time points postinfection (pi), supernatants were collected and cleared by centrifugation at 5,000g for 5 min, before HBeAg and HBs were determined on the Architect platform (Abbott, West Chicago, Illinois). Total DNA and RNA were purified from infected cells using the NucleoSpin® Tissue and RNA kits, respectively (Macherey Nagel, Düren, Germany). RNA was transcribed into cDNA using SuperScript III reverse transcriptase (Invitrogen, Carlsbad, California). HBV DNA (rcDNA and cccDNA) and RNA (pregenomic RNA, pgRNA) were quantified by real-time PCR on a LightCycler™ instrument (Roche Diagnostics, Mannheim, Germany) using specific PCR primers as described (Lucifora et al., 2014; Untergasser et al., 2006).

#### 4.8 | Purification and analysis of the human S-specific antibody MoMab

To produce the recombinant, anti-HBs antibody MoMab HEK 293 cells were transiently transfected and the antibody was purified by ion exchange chromatography from cell culture medium (InVivo Biotech Services, Berlin, Germany). Purified MoMab was separated by SDS-PAGE and stained with Coomassie Blue. For evaluation of EC50, ELISA was performed using immobilised HBs overlaid with MoMab. For neutralisation assay, HepG2-NTCP cells were infected as described above with HBV pre-incubated with MoMab (MOI of 500).

#### 4.9 | Synthesis and physicochemical characterisation of MoMab-conjugated to SPIONs

SPIONs were prepared from iron salt solutions by co-precipitation as described earlier (Shevtsov et al., 2015). The surfaces of the obtained nanoparticles were functionalised with MoMab antibody producing superparamagnetic conjugates so-called MoMab-SPIONs. To analyse the size distribution and nanoparticle size of SPIONs and MoMab-SPIONs, transmission EM and dynamic light scattering were performed. The hydrodynamic size and electrophoretic properties were measured on a Zetasizer Nano (Malvern Pananalytical, Malvern, UK). The NMR relaxation times of the  $R_2^*$ ,  $R_2$  and  $R_1$  coefficients were detected by a CXP-300 NMR-spectrometer (Bruker, Billerica, Massachusetts) with a magnetic field 7.1 Tessler. To assess the specific interaction of MoMab-SPIONs with HBs, the SPIONs and their obtained conjugates were co-incubated with recombinant HBsAg for 24 hr and the temporal  $T_2$  relaxation times were measured using the “switch assay” as described (Tassa, Shaw, & Weissleder, 2011).

#### 4.10 | Transmission electron microscopy (TEM)

HepG 2.2.15, HepAD38 cells and HBV-infected HepG2-NTCP cells (MOI of 100, experimental duration 9 days) were trypsinised and seeded into a 48-well plate using  $1 \times 10^5$  cells/ml. After 3 days pi, cells were incubated with SPIONs or MoMab-SPIONs for 3 hr, washed three times with PBS and fixed using 2.5% glutaraldehyde (EM grade) in 0.1 M sodium cacodylate buffer pH 7.4 (Science Services, Munich, Germany). Samples were post-fixed in 2% aqueous osmium tetroxide, dehydrated in gradual ethanol (30–100%) and propylene oxide followed by embedding in Epon (Merck, Darmstadt, Germany). Semithin sections were stained with toluidine blue, whereas the 50-nm ultra-thin sections (on 200 mesh copper grids) were stained with uranyl acetate/lead citrate. Images were documented by EM (Zeiss Libra 120 Plus, Carl Zeiss NTS GmbH, Oberkochen, Germany) combined with a Slow Scan charge-coupled device camera and analysed using the iTEM software (Olympus Soft Imaging Solutions, Münster, Germany).

#### 4.11 | S-CAR T-cell killing activity

HBV S-specific chimeric antigen receptor (S-CAR) was transduced into T-cells using retroviral vectors as described (Krebs et al., 2013). Huh-7 cells expressing SML, L or S after transient transfection were trypsinised, seeded into 96-well plates ( $3.5 \times 10^3$  cells per well) and cultured overnight before S-CAR T-cells ( $1 \times 10^6$  effector cells) were added. Cell viability was assessed over time for 4 days using the xCELLigence real-time cell analyser system and the RTCA software v1.2.1 (ACEA Biosciences, San Diego, California). To characterize T-cell activation, IFN- $\gamma$ , TNF- $\alpha$  and IL-2 levels were quantified in co-culture supernatants by ELISA (BioLegend, San Diego, California).

#### 4.12 | Animal experiments

Mice transgenic for LHBS (strain Alb-Psx; JAX stock # 027528; Chisari et al., 1986) or a 1.3-fold overlength HBV genome (strain HBV1.3.3.2; Guidotti et al., 1996) were bred in a specific pathogen-free animal facilities receiving human care. To evaluate, if MoMab specifically target HBs-expressing hepatocytes, 50  $\mu$ g and 100  $\mu$ g MoMab diluted in 100  $\mu$ l PBS were intravenously injected into Alb-Psx mice or C57BL/6 mice (as control); 4 hr after injection, mice were sacrificed, and blood and liver were collected. Binding of MoMab to hepatocytes in liver specimens was examined by IHC as described above. The study was conducted according to the German Law for the Protection of Animals with permission of the regulatory authority.

#### 4.13 | Image and statistical analysis

Image analysis was performed using the Java-based image processing program ImageJ 1.6.0 (NIH; Schneider et al., 2012). The structural

view of HBV S (PDB from van Hemert et al., 2008; van Hemert et al., 2008) was generated using PyMOL molecular graphics system, version 1.3 (Schrödinger, LLC). The student t-test statistical significance was calculated using GraphPad Prism, version 6.0c (GraphPad Software, San Diego, California).

## ACKNOWLEDGEMENTS

We thank Frank Thiele and Natalie Röder for their support with mouse experiments. We also thank Romina Bester and Hortenzia Jacobi for HBeAg and HBsAg measurement; Chunkyu Ko, Shanshan Luo and Yuchen Xia for fruitful discussions; and Jochen Wettengel for providing HBV virus stocks. We are also grateful to Dr. Boris P. Nikolaev and Yaroslav Marchenko for NMR measurements. Dr. Maxim Shevtsov was funded by the Ministry of Science and Higher Education of the Russian Federation (Agreement No. 075-15-2020-901). Open Access funding enabled and organized by Projekt DEAL.

## CONFLICT OF INTEREST

Ulrike Protzer and Karin Wisskirchen are co-founders and shareholders of SCG Cell Therapy holding the licence for the S-CAR and the bispecific antibody used in this study. The other authors declare no conflict of interest concerning the published work.

## AUTHOR CONTRIBUTIONS

**Lili Zhao:** Study and experiment design; performed experiment; data acquisition; data analysis; writing – original draft; writing – review and editing; final version approval. **Ulrike Protzer:** Study and experiment design; writing – original draft; writing – review and editing; final version approval. **Britta S. Möhl:** Study and experiment design; writing – original draft; writing – review and editing; final version approval. **Fuwang Chen:** Performed experiment; data acquisition; data analysis; writing – review and editing; final version approval. **Oliver Quitt:** Performed experiment; data acquisition; data analysis; writing – review and editing; final version approval. **Marvin Festag:** Performed experiment; data acquisition; data analysis; writing – review and editing; final version approval. **Marc Ringelhan:** Performed experiment; data acquisition; writing – review and editing; final version approval. **Julia Festag:** Performed experiment; data acquisition; writing – review and editing; final version approval. **Felix Bohne:** Performed experiment; data acquisition; data analysis; writing – review and editing; final version approval. **Michaela Aichler:** Performed experiment; data acquisition; writing – review and editing; final version approval. **Camille Sureau:** Data analysis; experimental tool; data interpretation; writing – review and editing; final version approval. **Maxim Shevtsov:** Data analysis; experimental tool; data interpretation; writing – review and editing; final version approval. **Maarten van de Klundert:** Data analysis; writing – original draft; writing – review and editing; final version approval. **Karin Wisskirchen:** Experimental tool; data interpretation; writing – review and editing; final version approval. **Volker Bruns:** Experimental tool; data interpretation; writing – review and editing; final version approval. **Frank Momburg:** Experimental tool; data interpretation; writing – review and editing; final version approval.

**Luidmila Yakovleva:** Performed experiment; data acquisition; writing – review and editing; final version approval.

## THE PAPER EXPLAINED

### Problem

Despite the availability of a prophylactic vaccine, Hepatitis B virus (HBV) infection remains a global health problem causing more than 880,000 deaths each year. Once chronic, the infection cannot be cured by the available antiviral treatments that target the viral polymerase, and patients remain at risk to develop hepatocellular carcinoma. Therefore, new therapeutic strategies and alternative therapeutic targets are urgently needed.

### Results

Our study shows that HBV envelope proteins that primarily are embedded into the endosomal membrane of infected hepatocytes become translocated to the plasma membrane. They can be detected on the surface of HBV-infected and HBV-replicating cells, in liver sections of HBV-transgenic mice and HBV-induced liver cancer. A novel, recombinant antibody confirmed the correct conformation of HBV envelope proteins on the cell surface and electron microscopy demonstrated their membrane distribution. Finally, we show that the envelope proteins can be recognised by redirected T-cells and allow targeting of infected hepatocytes by T-cell therapies using chimeric antigen receptors or T-cell engager antibodies.

### Impact

Our findings highlight that HBV envelope proteins are incorporated into the plasma membrane of infected hepatocytes and HBV-induced liver cancer cells where they provide an interesting target T-cell-based, potentially curative therapies.

## DATA AVAILABILITY STATEMENT

The data that support the findings of this study are available from the corresponding author upon reasonable request. The data that supports the findings of this study are available in the supplementary material of this article

## REFERENCES

- Bayer, K., Banning, C., Bruns, V., Wiltzer-Bach, L., & Schindler, M. (2016). Hepatitis C virus is released via a noncanonical secretory route. *Journal of Virology*, 90(23), 10558–10573. <https://doi.org/10.1128/JVI.01615-16>
- Berkower, I., Spadaccini, A., Chen, H., Al-Awadi, D., Muller, J., Gao, Y., ... Ni, Y. (2011). Hepatitis B virus surface antigen assembly function persists when entire transmembrane domains 1 and 3 are replaced by a heterologous transmembrane sequence. *Journal of Virology*, 85(5), 2439–2448. <https://doi.org/10.1128/JVI.02061-10>

- Bhatnagar, P. K., Papas, E., Blum, H. E., Milich, D. R., Nitecki, D., Karels, M. J., & Vyas, G. N. (1982). Immune response to synthetic peptide analogues of hepatitis B surface antigen specific for the a determinant. *Proceedings of the National Academy of Sciences of the United States of America*, 79(14), 4400–4404. <https://doi.org/10.1073/pnas.79.14.4400>
- Blumberg, B. S. (1977). Australia antigen and the biology of hepatitis B. *Science*, 197(4298), 17–25.
- Bohne, F., Chmielewski, M., Ebert, G., Wiegmann, K., Kurschner, T., Schulze, A., ... Protzer, U. (2008). T cells redirected against hepatitis B virus surface proteins eliminate infected hepatocytes. *Gastroenterology*, 134(1), 239–247. <https://doi.org/10.1053/j.gastro.2007.11.002>
- Brown, S. E., Howard, C. R., Steward, M. W., Ajdukiewicz, A. B., & Whittle, H. C. (1984). Hepatitis B surface antigen containing immune complexes occur in seronegative hepatocellular carcinoma patients. *Clinical and Experimental Immunology*, 55(2), 355–359.
- Busachi, C. A., Ray, M. B., & Desmet, V. J. (1978). An immunoperoxidase technique for demonstrating membrane localized HBsAg in paraffin sections of liver biopsies. *Journal of Immunological Methods*, 19(1), 95–99. [https://doi.org/10.1016/0022-1759\(78\)90012-1](https://doi.org/10.1016/0022-1759(78)90012-1)
- Chen, G. F., Wang, C., & Lau, G. (2017). Treatment of chronic hepatitis B infection-2017. *Liver International*, 37(Suppl 1), 59–66. <https://doi.org/10.1111/liv.13309>
- Chisari, F. V., Filippi, P., Buras, J., McLachlan, A., Popper, H., Pinkert, C. A., ... Brinster, R. L. (1987). Structural and pathological effects of synthesis of hepatitis B virus large envelope polypeptide in transgenic mice. *Proceedings of the National Academy of Sciences of the United States of America*, 84(19), 6909–6913.
- Chisari, F. V., Filippi, P., McLachlan, A., Milich, D. R., Riggs, M., Lee, S., ... Brinster, R. L. (1986). Expression of hepatitis B virus large envelope polypeptide inhibits hepatitis B surface antigen secretion in transgenic mice. *Journal of Virology*, 60(3), 880–887. <https://doi.org/10.1128/JVI.60.3.880-887.1986>
- Chisari, F. V., Klopchin, K., Moriyama, T., Pasquinelli, C., Dunsford, H. A., Sell, S., ... Palmiter, R. D. (1989). Molecular pathogenesis of hepatocellular carcinoma in hepatitis B virus transgenic mice. *Cell*, 59(6), 1145–1156.
- Chu, C. M., & Liaw, Y. F. (1995). Membrane staining for hepatitis B surface antigen on hepatocytes: A sensitive and specific marker of active viral replication in hepatitis B. *Journal of Clinical Pathology*, 48(5), 470–473.
- Debarry, J., Cornberg, M., & Manns, M. P. (2017). Challenges in warranting access to prophylaxis and therapy for hepatitis B virus infection. *Liver International*, 37(Suppl 1), 67–72. <https://doi.org/10.1111/liv.13320>
- Dreesman, G. R., Sanchez, Y., Ionescu-Matiu, I., Sparrow, J. T., Six, H. R., Peterson, D. L., ... Melnick, J. L. (1982). Antibody to hepatitis B surface antigen after a single inoculation of uncoupled synthetic HBsAg peptides. *Nature*, 295(5845), 158–160. <https://doi.org/10.1038/295158a0>
- Golsaz-Shirazi, F., Mohammadi, H., Amiri, M. M., Khoshnoodi, J., Kardar, G. A., Jeddi-Tehrani, M., & Shokri, F. (2016). Localization of immunodominant epitopes within the "a" determinant of hepatitis B surface antigen using monoclonal antibodies. *Archives of Virology*, 161(10), 2765–2772. <https://doi.org/10.1007/s00705-016-2980-y>
- Guidotti, L. G., Matzke, B., Pasquinelli, C., Shoenberger, J. M., Rogler, C. E., & Chisari, F. V. (1996). The hepatitis B virus (HBV) precore protein inhibits HBV replication in transgenic mice. *Journal of Virology*, 70(10), 7056–7061. <https://doi.org/10.1128/JVI.70.10.7056-7061.1996>
- Guidotti, L. G., Matzke, B., Schaller, H., & Chisari, F. V. (1995). High-level hepatitis B virus replication in transgenic mice. *Journal of Virology*, 69(10), 6158–6169. <https://doi.org/10.1128/JVI.69.10.6158-6169.1995>
- Hoffmann, J., Boehm, C., Himmelsbach, K., Donnerhak, C., Roettger, H., Weiss, T. S., ... Hildt, E. (2013). Identification of alpha-taxilin as an essential factor for the life cycle of hepatitis B virus. *Journal of Hepatology*, 59(5), 934–941. <https://doi.org/10.1016/j.jhep.2013.06.020>
- Huovila, A. P., Eder, A. M., & Fuller, S. D. (1992). Hepatitis B surface antigen assembles in a post-ER, pre-Golgi compartment. *The Journal of Cell Biology*, 118(6), 1305–1320.
- Inoue, J., Krueger, E. W., Chen, J., Cao, H., Ninomiya, M., & McNiven, M. A. (2015). HBV secretion is regulated through the activation of endocytic and autophagic compartments mediated by Rab7 stimulation. *Journal of Cell Science*, 128(9), 1696–1706. <https://doi.org/10.1242/jcs.158097>
- Jiang, B., Himmelsbach, K., Ren, H., Boller, K., & Hildt, E. (2015). Subviral hepatitis B virus filaments, like infectious viral particles, are released via multivesicular bodies. *Journal of Virology*, 90(7), 3330–3341. <https://doi.org/10.1128/JVI.03109-15>
- Kluge, B., Schlager, M., Pairan, A., & Bruss, V. (2005). Determination of the minimal distance between the matrix and transmembrane domains of the large hepatitis B virus envelope protein. *Journal of Virology*, 79(12), 7918–7921. <https://doi.org/10.1128/JVI.79.12.7918-7921.2005>
- Ko, C., Chakraborty, A., Chou, W. M., Hasreiter, J., Wettengel, J. M., Stadler, D., ... Protzer, U. (2018). Hepatitis B virus genome recycling and de novo secondary infection events maintain stable cccDNA levels. *Journal of Hepatology*, 69(6), 1231–1241. <https://doi.org/10.1016/j.jhep.2018.08.012>
- Krebs, K., Bottinger, N., Huang, L. R., Chmielewski, M., Arzberger, S., Gasteiger, G., ... Protzer, U. (2013). T cells expressing a chimeric antigen receptor that binds hepatitis B virus envelope proteins control virus replication in mice. *Gastroenterology*, 145(2), 456–465. <https://doi.org/10.1053/j.gastro.2013.04.047>
- Lambert, C., Doring, T., & Prange, R. (2007). Hepatitis B virus maturation is sensitive to functional inhibition of ESCRT-III, Vps4, and gamma 2-adaptin. *Journal of Virology*, 81(17), 9050–9060. <https://doi.org/10.1128/JVI.00479-07>
- Leistner, C. M., Gruen-Bernhard, S., & Glebe, D. (2008). Role of glycosaminoglycans for binding and infection of hepatitis B virus. *Cellular Microbiology*, 10(1), 122–133. <https://doi.org/10.1111/j.1462-5822.2007.01023.x>
- Lobaina, Y., & Michel, M. L. (2017). Chronic hepatitis B: Immunological profile and current therapeutic vaccines in clinical trials. *Vaccine*, 35(18), 2308–2314. <https://doi.org/10.1016/j.vaccine.2017.03.049>
- Lucifora, J., Xia, Y., Reisinger, F., Zhang, K., Stadler, D., Cheng, X., ... Protzer, U. (2014). Specific and nonhepatotoxic degradation of nuclear hepatitis B virus cccDNA. *Science*, 343(6176), 1221–1228. <https://doi.org/10.1126/science.1243462>
- Mangold, C. M., Unckell, F., Werr, M., & Streeck, R. E. (1995). Secretion and antigenicity of hepatitis B virus small envelope proteins lacking cysteines in the major antigenic region. *Virology*, 211(2), 535–543. <https://doi.org/10.1006/viro.1995.1435>
- Nakabayashi, H., Taketa, K., Miyano, K., Yamane, T., & Sato, J. (1982). Growth of human hepatoma cell lines with differentiated functions in chemically defined medium. *Cancer Research*, 42(9), 3858–3863. <https://cancerres.aacrjournals.org/content/42/9/3858.long>
- Ni, Y., Lempp, F. A., Mehrle, S., Nkongolo, S., Kaufman, C., Falth, M., ... Urban, S. (2014). Hepatitis B and D viruses exploit sodium taurocholate co-transporting polypeptide for species-specific entry into hepatocytes. *Gastroenterology*, 146(4), 1070–1083. <https://doi.org/10.1053/j.gastro.2013.12.024>
- Norder, H., Courouge, A. M., Coursaget, P., Echevarria, J. M., Lee, S. D., Mushahwar, I. K., ... Magnius, L. O. (2004). Genetic diversity of hepatitis B virus strains derived worldwide: Genotypes, subgenotypes, and HBsAg subtypes. *Intervirology*, 47(6), 289–309. <https://doi.org/10.1159/000080872>
- Qiu, X., Schroeder, P., & Bridon, D. (1996). Identification and characterization of a C(K/R)TC motif as a common epitope present in all subtypes

- of hepatitis B surface antigen. *Journal of Immunology*, 156(9), 3350–3356.
- Quitt, O., Luo, S., Meyer, M., Xie, Z., Golsaz-Shirazi, F., Loffredo-Verde, E., ... Protzer, U. (2021). T cell engager antibodies enable T cells to control HBV infection and to target HBsAg-positive hepatoma in mice. *Journal of Hepatology*, 75, 1058–1071. <https://doi.org/10.1016/j.jhep.2021.06.022>
- Roingard, P., & Sureau, C. (1998). Ultrastructural analysis of hepatitis B virus in HepG2-transfected cells with special emphasis on subviral filament morphogenesis. *Hepatology*, 28(4), 1128–1133. <https://doi.org/10.1002/hep.510280431>
- Safaie, P., Poongkunran, M., Kuang, P. P., Javaid, A., Jacobs, C., Pohlmann, R., ... Lau, D. T. (2016). Intrahepatic distribution of hepatitis B virus antigens in patients with and without hepatocellular carcinoma. *World Journal of Gastroenterology*, 22(12), 3404–3411. <https://doi.org/10.3748/wjg.v22.i12.3404>
- Schneider, C. A., Rasband, W. S., & Eliceiri, K. W. (2012). NIH image to ImageJ: 25 years of image analysis. *Nature Methods*, 9(7), 671–675.
- Schulze, A., Gripon, P., & Urban, S. (2007). Hepatitis B virus infection initiates with a large surface protein-dependent binding to heparan sulfate proteoglycans. *Hepatology*, 46(6), 1759–1768. <https://doi.org/10.1002/hep.21896>
- Schwarz, R. E., Wojciechowicz, D. C., Picon, A. I., Schwarz, M. A., & Paty, P. B. (1999). Wheatgerm agglutinin-mediated toxicity in pancreatic cancer cells. *British Journal of Cancer*, 80(11), 1754–1762. <https://doi.org/10.1038/sj.bjc.6690593>
- Sells, M. A., Chen, M. L., & Acs, G. (1987). Production of hepatitis B virus particles in Hep G2 cells transfected with cloned hepatitis B virus DNA. *Proceedings of the National Academy of Sciences of the United States of America*, 84(4), 1005–1009.
- Shevtsov, M. A., Nikolaev, B. P., Ryzhov, V. A., Yakovleva, L. Y., Marchenko, Y. Y., Parr, M. A., ... Multhoff, G. (2015). Ionizing radiation improves glioma-specific targeting of superparamagnetic iron oxide nanoparticles conjugated with cmHsp70.1 monoclonal antibodies (SPION-cmHsp70.1). *Nanoscale*, 7(48), 20652–20664. <https://doi.org/10.1039/c5nr06521f>
- Siegler, V. D., & Bruss, V. (2013). Role of transmembrane domains of hepatitis B virus small surface proteins in subviral-particle biogenesis. *Journal of Virology*, 87(3), 1491–1496. <https://doi.org/10.1128/JVI.02500-12>
- Stieler, J. T., & Prange, R. (2014). Involvement of ESCRT-II in hepatitis B virus morphogenesis. *PLoS One*, 9(3), e91279. <https://doi.org/10.1371/journal.pone.0091279>
- Sunami, Y., Ringelhan, M., Kokai, E., Lu, M., O'Connor, T., Lorentzen, A., ... Heikenwalder, M. (2016). Canonical NF-kappaB signaling in hepatocytes acts as a tumor-suppressor in hepatitis B virus surface antigen-driven hepatocellular carcinoma by controlling the unfolded protein response. *Hepatology*, 63(5), 1592–1607. <https://doi.org/10.1002/hep.28435>
- Sureau, C., & Salisse, J. (2013). A conformational heparan sulfate binding site essential to infectivity overlaps with the conserved hepatitis B virus a-determinant. *Hepatology*, 57(3), 985–994. <https://doi.org/10.1002/hep.26125>
- Tassa, C., Shaw, S. Y., & Weissleder, R. (2011). Dextran-coated iron oxide nanoparticles: A versatile platform for targeted molecular imaging, molecular diagnostics, and therapy. *Accounts of Chemical Research*, 44(10), 842–852. <https://doi.org/10.1021/ar200084x>
- Untergasser, A., Zedler, U., Langenkamp, A., Hosel, M., Quasdorff, M., Esser, K., ... Protzer, U. (2006). Dendritic cells take up viral antigens but do not support the early steps of hepatitis B virus infection. *Hepatology*, 43(3), 539–547. <https://doi.org/10.1002/hep.21048>
- van Hemert, F. J., Zaaijer, H. L., Berkhout, B., & Lukashov, V. V. (2008). Mosaic amino acid conservation in 3D-structures of surface protein and polymerase of hepatitis B virus. *Virology*, 370(2), 362–372. <https://doi.org/10.1016/j.virol.2007.08.036>
- Watanabe, T., Sorensen, E. M., Naito, A., Schott, M., Kim, S., & Ahlquist, P. (2007). Involvement of host cellular multivesicular body functions in hepatitis B virus budding. *Proceedings of the National Academy of Sciences of the United States of America*, 104(24), 10205–10210. <https://doi.org/10.1073/pnas.0704000104>
- World Health Organization. (2017). World Health Organization: GLOBAL HEPATITIS REPORT. <http://apps.who.int/iris/bitstream/handle/10665/255016/9789241565455-eng.pdf?sequence=1>.
- Yan, H., Zhong, G., Xu, G., He, W., Jing, Z., Gao, Z., ... Li, W. (2012). Sodium taurocholate cotransporting polypeptide is a functional receptor for human hepatitis B and D virus. *eLife*, 1, e00049. <https://doi.org/10.7554/eLife.00049>

## SUPPORTING INFORMATION

Additional supporting information may be found in the online version of the article at the publisher's website.

**How to cite this article:** Zhao, L., Chen, F., Quitt, O., Festag, M., Ringelhan, M., Wisskirchen, K., Festag, J., Yakovleva, L., Sureau, C., Bohne, F., Aichler, M., Bruss, V., Shevtsov, M., van de Klundert, M., Momburg, F., Möhl, B. S., & Protzer, U. (2021). Hepatitis B virus envelope proteins can serve as therapeutic targets embedded in the host cell plasma membrane. *Cellular Microbiology*, 23(12), e13399. <https://doi.org/10.1111/cmi.13399>